Springer

KSME

Journal of Mechanical Science and Technology 25 (3) (2011) 703~711
www.springerlink.com/content/1738-494x
DOI 10.1007/s12206-011-0118-4

An efficient CFD-based method for aircraft icing simulation using a reduced order model †

Sung Ki Jung[1], Sungmin Shin[1], Rho Shin Myong[2,*] and Tae Hwan Cho[2]

[1]*School of Mechanical and Aerospace Engineering, Gyeongsang National University, Gyeongnam, Jinju, 660-901 Korea*
[2]*School of Mechanical and Aerospace Engineering, Research Center for Aircraft Parts Technology, Gyeongsang National University, Gyeongnam, Jinju, 660-901, Korea*

(Manuscript Received June 7, 2010; Revised December 2, 2010; Accepted December 30, 2010)

Abstract

In-flight icing is a critical technical issue for aircraft safety and, in particular, the droplet impingement areas on aircraft surfaces must be investigated for anti-/de-icing devices. As a step toward the prediction of droplet impingement on aircraft, an Eulerian-based droplet impingement code that provides collection efficiency for air flows around an airfoil containing water droplets is developed. A computational fluid dynamics (CFD) solver was also developed to solve the clean airflow. Then, a proper orthogonal decomposition (POD) method, a reduced order model (ROM), that optimally captures the energy content from a large multi-dimensional data set is utilized to efficiently predict the collection efficiency and ice accretion shapes on an airfoil following the mean volume diameter, liquid water contents and angle of attacks. As a result it is shown that the collection efficiency and ice shapes were in good agreement with the simulated and predicted results.

Keywords: CFD; Eulerian; Droplet impingement; Ice accretion; Proper orthogonal decomposition

1. Introduction

Protection of aircraft from the adverse effects of ice accretion is a crucial design problem, because ice accretion on critical aerodynamic surfaces can significantly deteriorate aircraft performance and safety. Ice protection systems are employed on most commercial aircraft to reduce or eliminate the adverse effects of ice accretion. The design of ice protection systems requires knowledge of local and total droplet impingement intensities and limitations in order to determine the energy levels per unit area for ice protection and the extent of the surface area to be protected. Those concerns have been conducted by experimental and analytical studies of the in-flight icing problems. Since the 1940s, experimental and flight tests have been conducted for protection systems and investigation of their aerodynamic effectiveness. However, significant progress in the theoretical studies only came later in the 1970s with the advent of the computer. The main contributors to the experimental and theoretical research initially were the NASA Glenn Research Center in the USA, DERA in the UK and ONERA in France. Since the early 1990s, a number of countries have been involved in the field of aircraft icing, and most notably Canada is now leading the way in the development of second and third generation analysis tools, such as the FENSAP-ICE package [1-4].

Numerical simulations have been traditionally based on inviscid panel or Euler plus boundary layer correction computations for the air flow and on Lagrangian particle tracking techniques for the droplet Impingement, such as the NASA LEWICE and ONERA codes. However, if the compressible Navier-Stokes equations are solved, the influence of the viscous effects can be taken into consideration completely. It would be more natural to compute the droplet impingement on airfoils using an Eulerian approach rather than the Lagrangian model [8]. Furthermore the Eulerian approach is more flexible for three-dimensional complex geometries [5]. Despite improvements in the theoretical approaches and the use of computers, a whole computation considering flight and icing conditions under FAR 25 Appendix C [6] is still a computationally time-consuming problem. Instead of a whole computation, an alternative approach to this issue is the use of meta-modeling strategies from the output of a high-fidelity analysis tool at discrete points in the design space, such as the icing conditions in FAR 25 Appendix C. Among the available meta models, reduced order model (ROM) based on properties of the proper orthogonal decomposition (POD) to characterize an

† This paper was recommended for publication in revised form by Associate Editor Gihun Son

* Corresponding author. Tel.: +82 55 751 6107, Fax.: +82 55 757 5622
E-mail address: myong@gnu.ac.kr

ensemble of simulation results was adopted. The POD method has been used extensively in the fields of random variables, image processing, data compression and system controls. In fluid mechanics POD was first introduced by Lumley [16]. The POD provides an efficient method of capturing the dominant features of the multi degrees of the freedom system and represents the desired precision using a relevant set of modes, thus reducing the order of the system.

In this study the compressible Navier-Stokes code was developed as a step prior to droplet particle tracking, and the Eulerian-based droplet impingement code was also developed to obtain the impingement intensities and limitations on airfoils that result from the supercooled water droplets. In order to predict the ice shapes following the angle of attacks, mean volume diameter (MVD) and liquid water contents (LWC) under FAR 25 Appendix C, the POD was applied using an ensemble of x and y coordinate values of the ice shapes.

2. Numerical method

In order to calculate the flow fields around the airfoil, two-dimensional compressible Navier-Stokes equations based on the finite volume method (FVM) was developed. The Spalart-Allmaras model was employed as the turbulence model for the Reynolds Average Navier-Stokes (RANS) equations. A droplet impingement solver based on an Eulerian approach augmented by droplet-related continuity and momentum equations was also developed. It solves the fine-grain partial differential equations for the droplet velocity and concentration throughout the flow field. Furthermore, it yields distributions of the collection efficiency, impingement patterns, and shadowing limits for droplets over arbitrarily complex geometry.

2.1 CFD solver

In order to simulate the droplet impingement, the air flow should be computed prior to the simulation. The classical compressible Navier-Stokes equations were employed as the governing equations. The system of governing equations can be written in the following integral and conservative form:

$$\frac{\partial}{\partial t}\int_{\Omega}\vec{W}_a d\Omega + \int_{\partial\Omega}\left(\vec{F}_{a,c}-\vec{F}_{a,v}\right)dS = 0\,. \tag{1}$$

In general the mass loading ratio of the bulk density of the droplets over the bulk density of the air is in the order of 10^{-3} for icing conditions. Therefore one-way coupling in which the droplet flows do not affect the air flows may be considered valid in the present problem.

The CFD solver is formulated for a finite control volume and solved using an explicit time marching procedure. For the spatial discretization Roe's approximate Riemann solver and Van Leer's monotone upstream-centred schemes (MUSCL) was employed. Van Albada's limiter was adopted in order to prevent the generation of oscillation and preserve the monotonicity. For the temporal discretization, an explicit scheme based on the fifth stages Runge-Kutta scheme was employed. The local time step was adopted to accelerate the convergence. In order to simulate the turbulent effect in flow fields, RANS was employed and the Spalart-Allmaras turbulent model was chosen to close the RANS. For the boundary conditions no-slip and Riemann invariant conditions were applied on the solid surface and the far-fields. An ideal gas equation was also employed to close the system of equations [7].

2.2 Droplet impingement solver

The governing equations of the droplet impingement are based on the Eulerian model proposed by Bourgault et al. [8], which is briefly reviewed here. This is essentially a two-fluid model consisting of the set of Navier-Stokes equations augmented by droplet-related continuity and momentum equations. For the air-droplets flows, the following assumptions are considered for in-flight icing situations: the droplets are spherical without any deformation or breaking; there is no droplets collision, coalescence or splashing; there is no heat and mass exchange between the droplets and the surrounding air; the turbulence effects on the droplets can be neglected; the only forces acting on the droplets are due to air drag, gravity and buoyancy. The droplet impingement solver is based on the FVM in order to directly implement the grid topologies of the CFD solver. The system of governing equations can be written in the following integral and conservative form:

$$\frac{\partial}{\partial t}\int_{\Omega}\vec{W}_D d\Omega + \int_{\partial\Omega}\vec{F}_D dS = \int_{\Omega}\vec{Q}_D d\Omega\,, \tag{2}$$

where W_D, F_D, and Q_D are the conservative variables, a convective flux, and a source term, respectively.

$$\vec{W}_D = \begin{bmatrix}\alpha\\ \alpha u_D\\ \alpha v_D\end{bmatrix},\quad \vec{F}_D = \begin{bmatrix}\alpha V_D\\ \alpha u_D V_D\\ \alpha v_D V_D\end{bmatrix}, \tag{3}$$

$$\vec{Q}_D = \begin{bmatrix} 0\\ \dfrac{C_D \mathrm{Re}_D}{24K}(u_a-u_D)\alpha\\ \dfrac{C_D \mathrm{Re}_D}{24K}(v_a-v_D)\alpha + \left(\dfrac{\rho_w-\rho_a}{\rho_w Fr^2}\right)g\alpha \end{bmatrix}. \tag{4}$$

The source term of the momentum equation accounts for the gravity and buoyancy effects. C_D is a drag coefficient for spherical droplets.

$$C_D = \begin{cases} \dfrac{24\left(1+0.15\,\mathrm{Re}_D^{0.687}\right)}{\mathrm{Re}_D}, & \text{if} \quad \mathrm{Re}_D \le 1300\\ 0.4\,, & \text{Otherwise}\end{cases} \tag{5}$$

where $\mathrm{Re}_D=\rho_w d U_{a,\infty}|V_a-V_D|/\mu$. In Eq. (4) K and the Fround

number are defined as:

$$K = \rho d^2 U_{a,\infty} / 18 L_\infty \mu \,, \quad Fr = U_{a,\infty} / \sqrt{Lg} \,. \tag{6}$$

An important parameter that controls the ice accretion on a solid surface is the local collection efficiency β which is the normalized flux of water on the solid surface. The droplet solution yields α and V_D throughout the solution domain, and the surface collection efficiency β can then be calculated as:

$$\beta = -\alpha \vec{V}_D \cdot \vec{n} \,, \tag{7}$$

where $\vec{n}$ is a normal vector on solid surface. Droplet impinges on the solid surface when $V_D \cdot \vec{n}$ is positive, whereas droplet does not impinge on the solid surface when $V_D \cdot \vec{n}$ is negative. In order to simulate the air-droplet flows, the convective flux was discretized using a first-order upwind scheme. Explicit time-stepping was also employed as a temporal discretization. For the boundary conditions no-slip and Riemann invariant conditions were applied on the solid surface and far-fields.

2.3 Ice accretion solver

Ice accretion is mainly divided in two types due to the icing conditions: rime and glaze icing. For the rime, the shear stress and heat flux are not considered since the droplet is iced immediately when the droplet impingement occurs on the solid surface. However, droplets in the glaze condition move in a streamlined direction. Therefore, the shear stress and heat flux should be considered. This means that the Navier-Stokes equation should be calculated to employ the shear stress and heat flux in the ice accretion solver. In this study, the rime ice solver was developed using a simple ice accretion model based on the control volume. For the glaze ice, the ICE3D, a sub-module of FENSAP commercial code, was used to simulate ice accretion on the surface [9, 10]. ICE3D consists of converting the classical Messinger model into a partial difference equation system of conservation equations, thus, allowing a natural extension from two to three dimensions. The resulting system of PDE is the mass and energy conservation. From the Eulerian droplet solver, collection efficiency and droplet velocity are provided to ICE3D, and CFD solver provides the local wall shear stress and convective heat flux.

The rime ice forms in an environment with a low temperature and supercooled water droplets freeze instantaneously when they impinge on the solid surface. Therefore, the ice volume, V_{ICE}, can be calculated as [11]:

$$V_{Ice} = \frac{m_{Water} \cdot \Delta t}{\rho_{ice}} \,, \tag{8}$$

where m_{Water}=$LWC \cdot U_{a,\infty} \cdot \beta \cdot A$ and m_{Water} is defined by liquid water contents (LWC), velocity, collection efficiency and droplet impingement area. Finally ice volume is calculated using m_{Water}, density of ice and time. Droplet impingement area is already known. The height of ice accretion is therefore determined. The LWC means the amount of water contained in the cloud.

According to the ice volume, the ice shape after a time step can be predicted with the assumption that ice grows in the direction normal to the airfoil surface. When the airfoil shape is changed by ice accretion, it results in the air flow-field. Therefore, the air flow-field needs to be solved again. The new ice shape can then be predicted by replacing the old collection efficiency with new collection efficiency after solving the droplet impingement again. The final shape of the ice accretion can be obtained by repeating this iterative process over a number of time steps until the end of the ice accretion time.

3. Reduced-order model: snapshot of POD

The POD is a procedure that provides an optimal orthonormal set of basis vectors for a given ensemble of data. The objective is to find a vector, Φ, of length n for an ensemble of data, $Y = \{Y_1, Y_2, \cdots, Y_m\}$, where $Y_i = \{y_{i1}, y_{i2}, \cdots, y_{in}\}$. For practical calculations, the number of FAR 25 Appendix C, n can be very large and the solution of the corresponding eigenvalue problem can be prohibitively expensive. In order to avoid this computation Sirovich [12] introduced the method of snapshots. In this method, instead of solving an n x n matrix for the eigen system, an N x N matrix, where N is the number of snapshots in the ensemble of data, needs to be dealt with,

$$CV = \lambda V \,, \tag{9}$$

where

$$C_{ij} = \frac{1}{N} Y_i^T Y_j \,,$$

and

$$V = \left[v_1, v_2, \cdots v_N \right]^T \,. \tag{10}$$

Then the POD basis modes may be written in terms of the members of the ensemble data and eigenvector of the correlation matrix C as:

$$\Phi = \sum_{i=1}^{N} v_i Y^{(i)} \,. \tag{11}$$

Among every POD basis mode, only M of the available modes can be chosen by prescribing an energy level, e, in a percentage such that:

$$\sum_{i=1}^{M} \lambda_i \Big/ \sum_{j=1}^{N} \lambda_j > e \,. \tag{12}$$

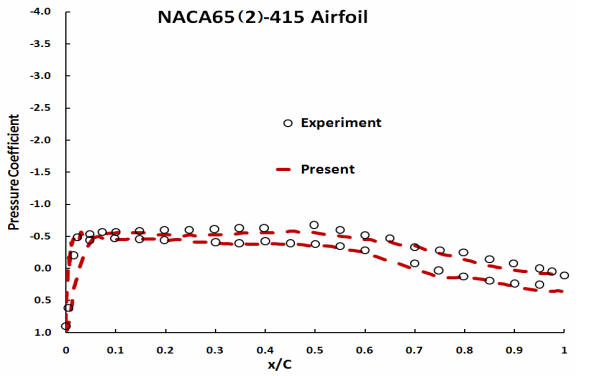

Fig. 1. Comparison of pressure distribution between the experimental data and present solution.

A reduced-order model with a reduced subspace defined by an energy level, $Y^{POD} = Span\{\Phi_1, \Phi_2, \cdots, \Phi_M\}$, can be obtained from expressing each state as:

$$Y = Y_{ave} + y_i = Y_{ave} + \sum_{i=1}^{M} a_i' \Phi_i \quad , \tag{13}$$

where Y_{ave} is the average value of the dataset over all the snapshots, Φ_i is the i^{th} POD basis mode, and the POD coefficients, a_i', are determined as a function of the varying parameters as follows:

$$a_i' = \left(\frac{y_i \Phi_i}{\Phi_j \Phi_i} \right). \tag{14}$$

The use of reduced order models based upon the POD to predict the ice shape on a solid surface requires the transformation of the projection coefficients, a_i', from the discrete sample space to a continuous space. If a_i' varies as a smooth function with the change in parameters, then a meta-model may be used to determine the POD projection coefficients at intermediate parametric values not included in the original data ensemble [13]. In this study a piecewise linear interpolation was adopted to predict the collection efficiency and ice shapes on the solid surface following the FAR 25 Appendix C and the angle of attacks.

4. Validation

Two test cases from the literature were selected to validate the CFD and droplet impingement solver. The first case is pressure distributions of a NACA $65_2$415 airfoil for clean air flows. An experimental test [14] was conducted in the two dimensional test section of the NASA icing research tunnel (IRT) on a NACA $65_2$415 airfoil to obtain the aerodynamic data. The Mach and Reynolds number are 0.23 and 4.9×10^6 respectively. The numerical simulation was conducted using the commercial grid generation package GRIDGEN. The grid topology is a C-type and structured grid; its size is 421 x 65.

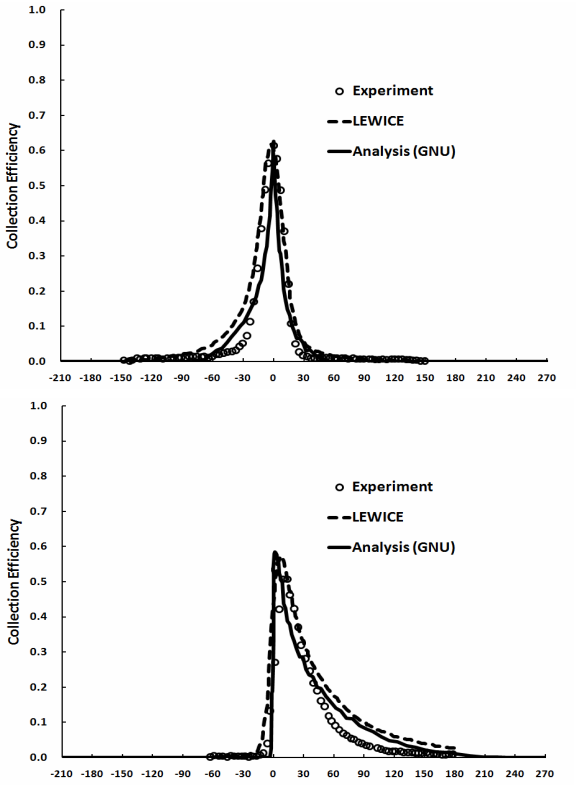

Fig. 2. Comparison of the collection efficiency of the experimental, LEWICE and present result (up: AoA 0 degree; down: AoA 8 degree).

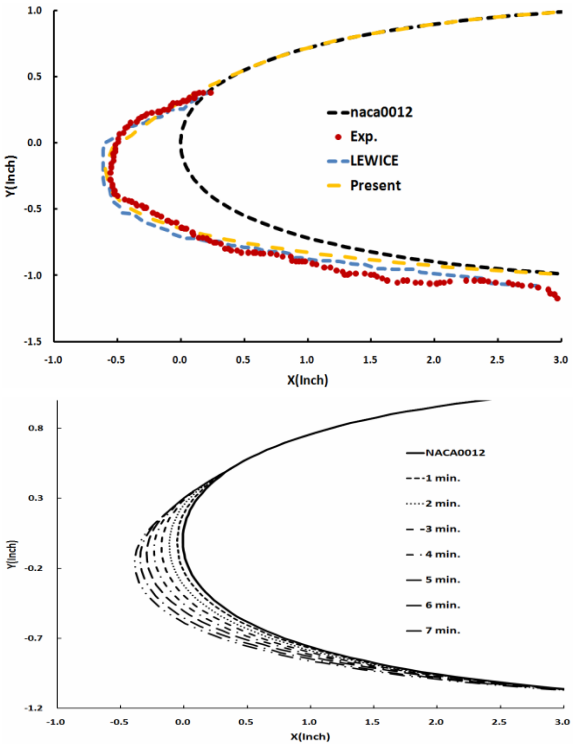

Fig. 3. Comparison of the ice shapes of on the experimental data, LEWICE, and present solution (up) and temporal variation of ice shapes (down).

No slip and Riemann invariant conditions were applied on the solid surface and far field, respectively. Also ρ_∞, V_∞ and E_∞ were applied as initial conditions. Fig. 1 shows comparisons of the pressure distribution between the experimental data and present solutions on the airfoil. The pressure distributions were in good agreement. The second case is collection efficiencies for a NACA 65_2415 airfoil for droplet impingement. The collection efficiency is the droplet impingement intensities and limitation: This is an important parameter that controls the ice accretion on the surface. An experimental test [14] was conducted in the NASA Glenn IRT. A CCD camera and laser were used to measure the droplet impingement on an airfoil. The MVD, Mach, and Reynolds numbers were 21 micrometers, 0.23, and 4.9×10^6, respectively. A numerical simulation based on the Eulerian approach was conducted using the same grid together with the C-type and structured grid which is employed in the CFD solver.

Fig. 2 shows the comparisons of the collection efficiencies among the experimental data, LEWICE, and present solutions on the airfoil. The collection efficiencies were in good agreement with each other. The collection efficiency in Fig. 2 shows the effectiveness of the angle of attack. Droplet impingement limits were moved from the upper surface to the lower surface. For the angles of attack, 8 degree, the range of the droplet impingement limits was reduced to approximately 25 percent and increased to approximately 360 percent more than an angle of attack, 0 degree, from the leading edge on the upper and lower surfaces, respectively.

Fig. 3 shows a comparison of the ice shapes between experimental data and present solution around the leading edge of NACA 0012 airfoil. In this study each solver is assumed quasi-steady state. Therefore fully converged air and droplet solutions are applied to ice accretion solver. Calculations of ice accretions are repeated every 10 second. The total time exposed in icing condition is 7 minutes, thus total 42 iterations using CFD, droplet impingement and ice accretion solvers. Experimental tests [15] were also conducted in the NASA IRT. The ice shapes were observed to be in good agreement with each other. In order to install the ice protection system, droplet impingement limits considering the effectiveness of the angle of attack must be investigated in the FAR 25 Appendix C. Once all points in icing conditions need to be calculated, it is still a computationally time-consuming problem. In order to avoid these cumbersome computations, the ROM can be an alternative method as meta model. The next section describes the application of the POD to efficiently capture the collection efficiencies and ice shapes.

5. Application

The POD method was applied to predict the collection efficiency and ice shape. At first, a model containing 42 basis vectors (collection efficiencies at 42 cases) was selected as samples for snapshots of the POD. The model consists of the collection efficiencies on the solid surface at a Mach number of 0.3, angles of attacks from zero to six degrees, and an MVD of fifteen to forty micrometers. The sample points for the meta model are summarized in Table 1.

Table 1. Samples of the snapshot.

AoA (°)	MVD (μm)	Snapshot
0	15	1
	20	2
	25	3
	30	4
	35	5
	40	6
6	40	42

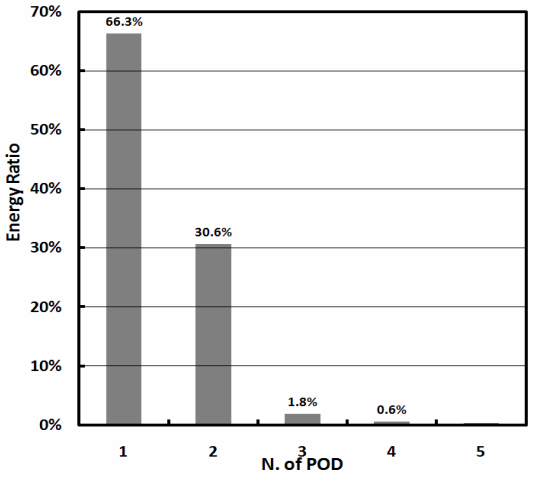

Fig. 4. Captured energy ratio vs the number of POD modes.

Fig. 4 shows the variation of the energy captured by the POD modes against the number of POD modes. Most energy over 99 percent is captured within the first four modes. It indicates that the dataset is sufficient to capture the collection efficiencies. While the energy captured by a given set of basis functions provides some understanding of the relative accuracy of the model, the actual error remains unknown. This quantity can be calculated by comparing the original data with the reconstructed data generated by the ROM.

Fig. 5 shows the variation of the reconstructed data varying with the number of POD modes. While the first POD mode, which is the most dominant mode, is well predicted regarding the impingement intensity, it is not sufficient to obtain the droplet impingement limit and slope of the collection efficiency. As the modes are increased, further improvements are obtained, and the detail of the collection efficiency is more clearly represented than in one mode. The data plotted in Fig. 5 suggest that there is almost no difference between the original and reconstructed solutions using only four of the available POD modes. The POD modes corresponding coefficients were employed to predict the collection efficiency for unknown icing conditions. In order to compose a meta model,

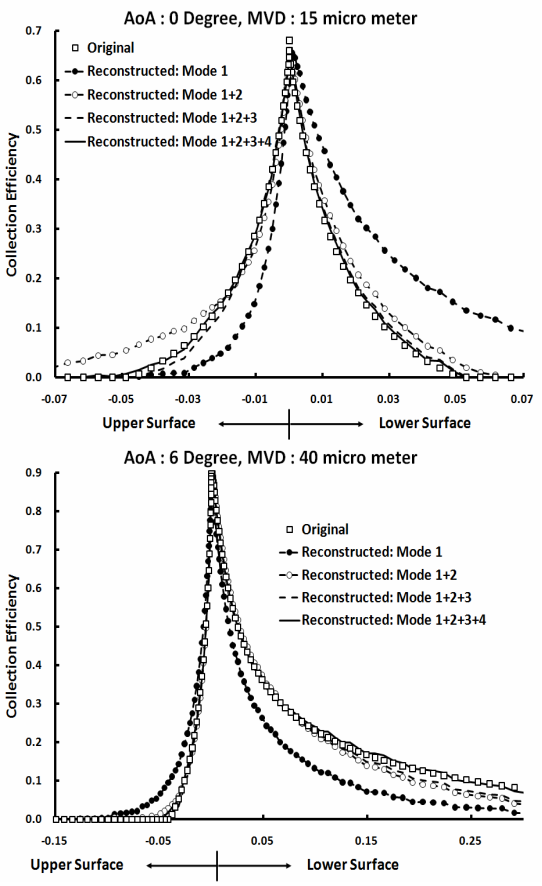

Fig. 5. Comparisons of original and reconstructed data with dominant POD modes.

the POD coefficients of the discretized snapshot samples were replaced with continuous space using a piecewise linear interpolation for each mode.

Fig. 6 shows that the discretized snapshot samples following the angles of attack and MVDs are replaced with the continuous space in the first four modes. With the meta model and POD modes, the predictions of the collection efficiencies were compared with the simulation data of droplet impingement.

Fig. 7 shows the comparisons of the simulated and predicted data using a droplet impingement solver and a meta model of the POD. It was observed that the collection efficiencies are in good agreement with each other. Using the

POD method, a shape of ice accretion can be predicted based on the same approach. The same approach that was applied to predict the collection efficiency was employed to predict the ice shapes. A model containing 24 basis vectors was selected as samples for the snapshot of POD. The model consists of the ice shapes around the leading edge on airfoils at a Mach number of 0.3, a temperature of -10 Celsius, angles of attacks every two degrees from zero to six degrees, and various LWCs and MVDs. In the process, most energy over 99 percent was captured within the first three modes. Also, the POD modes corresponding coefficients were employed to

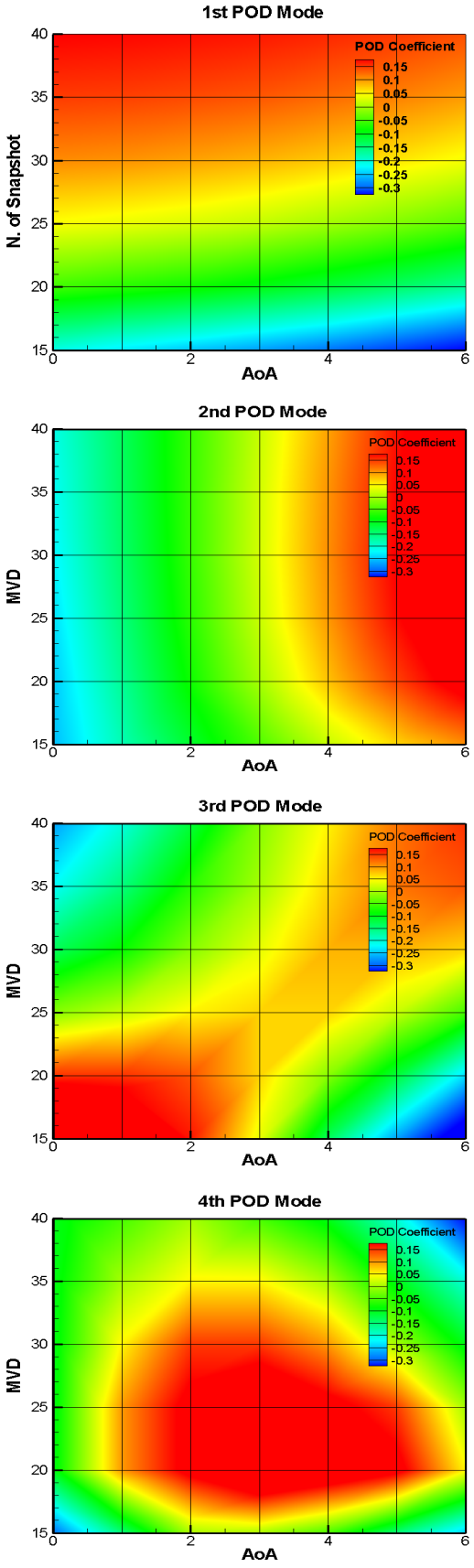

Fig. 6. Meta models on POD coefficients of first four POD modes.

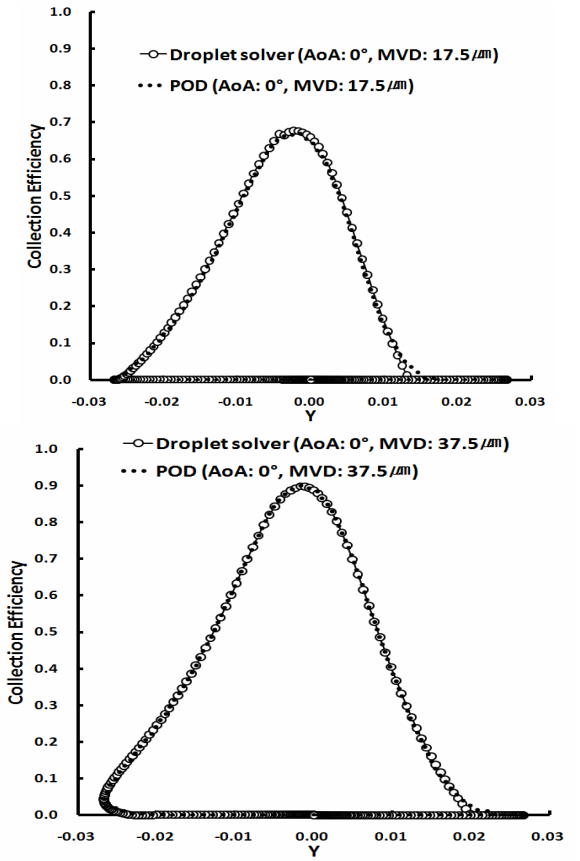

Fig. 7. Comparisons between the solutions of droplet solver and POD of collection efficiency.

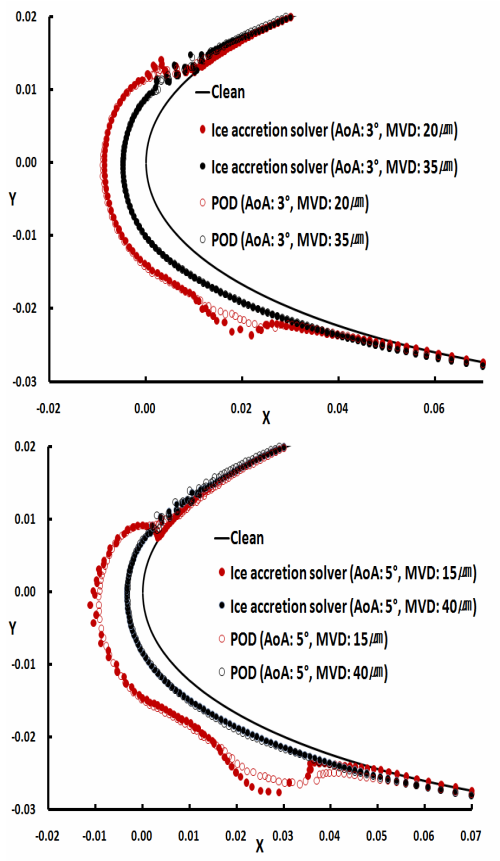

Fig. 8. Comparisons between the solutions of ice accretion solver and POD of ice shapes.

predict the shapes of ice for the unknown icing conditions. In order to compose a meta model, the POD coefficients of the discretized snapshot samples were placed into continuous space using piecewise linear interpolation for each mode. With the meta model and POD modes, the predictions of the ice shapes were compared with the simulation data of ice accretion.

Fig. 8 shows the comparisons of the simulated and predicted data using an ice accretion solver and the meta model of the POD. For the MVD, 35 and 40 micrometers, ice shapes were well reconstructed, with an excellent capture of the ice thickness and the location. For the MVD, 15 and 20 micro meters, small differences between the locations of the groove were observed at the lower surface.

6. Conclusions

Eulerian-based droplet impingement and ice accretion codes that provide the collection efficiency and shapes of ice for air flows around an airfoil containing water droplets were developed. A CFD code was also developed to solve the clean flows. Both methods were compared with the experimental data. The pressure distributions, collection efficiencies, and ice shapes were in good agreement with the experimental and present results. The developed codes were applied to icing conditions under FAR 25 Appendix C. However, a whole computation for icing conditions is still a computationally time-consuming problem. As an alternative approach, the ROM based on properties of the POD method to characterize the ensemble of simulation results was adopted to predict the collection efficiencies and ice shapes. For the collection efficiency, energy over 99 percent was captured within the first four modes from 42 snapshot samples. A reconstruction using four of the available modes was compared with the original data, and it was shown that the collection efficiencies were in good agreement. In order to compose the meta model, the POD coefficients were utilized to replace the discretized snapshot samples with a continuous space using a piecewise linear interpolation. The same approach predicting the collection efficiency was employed to predict the ice shapes. A model containing 24 basis vectors was selected as samples for the snapshot of the POD. Most energy over 99 percent was captured within the first three modes. With the meta model utilizing POD coefficients and modes, the predictions of ice shapes were compared with the simulation data of the ice accretion. As a result, the collection efficiencies and ice shapes were in good agreement with the simulated and predicted data. In the future, the aerodynamic ef-

fectiveness due to ice accretion will be investigated using the POD method, and the development of three dimensional ice analysis system is required to investigate the three dimensional effectiveness on the ice accretion.

Acknowledgment

This work supported by the KARI under KHP Dual-Use Component Development Program funded by the MKE and Priority Research Centers Program through the National Research Foundation of Korea funded by the Ministry of Education, Science and Technology (2010-0029690), South Korea.

Nomenclature

$\vec{W}_a$	:	Conservative variables for clean air flow
$\vec{F}_{a,c}$	:	Convective flux for air flow
$\vec{F}_{a,v}$	:	Viscous flux for air flow
$\vec{W}_D$	:	Conservative variables for droplet
$\vec{F}_D$	:	Convective flux for droplet
$\vec{Q}_D$	:	Source term for droplet
$\vec{n}$	:	Normal vector
Ω	:	Control volume
α	:	Volume fraction of water
β	:	Collection efficiency
u_a	:	Air velocity for x-component
u_D	:	Droplet velocity for x-component
v_a	:	Air velocity for y-component
v_D	:	Droplet velocity for y-component
L	:	Characteristic length
V_a	:	Contravariant velocity for clean air flow
V_D	:	Contravariant velocity for droplet
$U_{a,\infty}$	:	Speed of air at infinity
C_D	:	Drag coefficient for spherical droplet
Re_d	:	Droplet Reynolds number
ρ_w	:	Density of water
ρ_a	:	Density of air
ρ_{ice}	:	Density of ice
m_{Water}	:	Mass of water
V_{Ice}	:	Volume of ice accretion
A	:	Impingement area on the surface
Fr	:	Froude number
g	:	Gravity
μ	:	Dynamic viscosity of air
C	:	Correlation matrix
V	:	Eigenvector
λ	:	Eigenvalue
N	:	Number of snapshot
Y	:	Snapshot sample
e	:	Energy ratio
a'	:	POD Coefficient
Φ	:	POD basis mode

References

[1] R. W. Gent, N. P. Dart and J. T. Cansdale, Aircraft Icing, *Phil. Trans. R. Soc. Lond.*, 358 (2000) 2873-2911.

[2] M. B. Bragg, A. P. Broeren and L. A. Blumenthal, Iced-Airfoil Aerodynamics, *Progress in Aerospace Sciences*, 41 (2005) 323-362.

[3] F. T. Lynch and A. Khodadoust, Effects of Ice Accretions on Aircraft Aerodynamics, *Progress in Aerospace Sciences*, 37 (2001) 669-767.

[4] R. J. Kind, M. G. Potapczuk, A. Feo, C. Golia and A. D. Shah, Experimental and Computational Simulation of In-Flight Icing Phenomena, *Progress in Aerospace Sciences*, 34 (1998) 257-345.

[5] S. K. Jung, S. M. Shin, R. S. Myong, T. H. Cho, H. H. Jeong and J. H. Jung, Ice Accretion Effect on the Aerodynamic Characteristics of KC-100 Aircraft, *AIAA 2010-1237* (2010).

[6] K. Nakakita, S. Nadarajah and W. Habashi, Toward Real-Time Aero-Icing Simulation of Complete Aircraft via FENSAP-ICE, *Journal of Aircraft*, 47 (1) (2010) 96-109.

[7] J. Blazek, *Computational Fluid Dynamics: Principles and Application*, Elsevier (2005).

[8] Y. Bourgault, W. G. Habashi, J. Dompierre and G. S. Baruzzi, A Finite Element Method Study of Eulerian Droplets Impingement Models, *Int. J. Numer. Meth. Fluids*, 29 (1999) 429-449.

[9] H. Beaugendre, F. Morency and W. G. Habashi, FENSAP-ICE's Three-Dimensional In-Flight Ice Accretion Module: ICE3D, *Journal of Aircraft*, 40 (2) (2003) 239-247.

[10] *NTI Solutions User Manual*, Newmerical Technologies Int., (2008).

[11] Y. Cao, Q. Zhang and J. Sheridan, Numerical Simulation of Rime Ice Accretions on an Aerofoil Using an Eulerian Method, *The Aeronautical Journal*, 112 (1131) (2008) 243-249.

[12] L. Sirovich, Turbulence and the Dynamics of Coherent Structures, Part 1 : Coherent Structures, *Quarterly of Applied Mathematics*, 45 (3) (1987) 561-571.

[13] M. Mifsud, S. Shaw and J. Bennett, A Meta-Modeling Technique Using POD in Parametric Studies of Weapon Aerodynamics, *AIAA 2006-6005* (2006).

[14] M. Papadakis, K. E. Hung, G. T. Vu, H. W. Yeong, C. S. Bidwell, M. D. Breer and T. J. Bencic, Experimental Investigation of Water Droplet Impingement on Airfoils, Finite Wings, and an S-Duct Engine Inlet, *NASA-TM-2002-211700* (2002).

[15] M. Vargas, M. Papadakis, M. Potapczuk, H. Addy, D. Sheldon and J. Giriunas, Ice Accretions on a Swept GLC-305 Airfoil, *NASA-TM-2002-211557* (2002).

[16] J. L. Lumley, The Structure of Inhomogenous Turbulent Flows in Atmospheric Turbulence and Wave Propagation, *A. M. Yaglom and V. I. Tatarski, eds.*, Nauka, Moscow (1967) 166-178.

Sung Ki Jung received his B.S. degree in Mechanical and Aerospace Engineering from Gyeongsang National University, South Korea in 2003. He then received his M.S. degree from the same department of GNU in 2006. S. K. Jung is currently a Ph.D. candidate in GNU.

Rho Shin Myong received the B.S. and M.S. degrees in the dept. of aeronautical engineering from the Seoul National University in 1987 and 1989, respectively. He received a Ph.D. degree in the dept. of aerospace engineering from the University of Michigan in 1996. He worked at the NASA Goddard Space Flight Center from 1997 to 1999. Currently, he is a professor of the department of aerospace and system engineering at the Gyeongsang National University. He is an associate editor of the Communications in Computational Physics and an editorial board member of the International Journal of Computational Fluid Dynamics.

Tae Hwan Cho majored Aerospace Engineering and received B.S. in the Seoul National University, Korea, in 1969, and M.S. in the Northrop University, U.S.A. in 1974, and Ph D. in the University of Maryland, U.S.A. in 1985. He worked as an academic faculty member at the R.O.K. Airforce Academy from 1969-1973, and as a researcher at the Agency for Defence Development of Korea from 1973 to 2000. He served as a President for the Korean Society for Aeronautical and Space Sciences, 1999-2001. Currently, he is a professor of the Department of Aerospace and System Engineering at the Gyeongsang National University.